Transactions of KSAE, Vol. 33, No. 10, pp.777-788 (October, 2025)

pISSN 1225-6382 / eISSN 2234-0149
DOI http://dx.doi.org/10.7467/KSAE.2025.33.10.777

Study on Adsorption Performance of Activated Carbon Canister for Flow Rate and Concentration of Adsorbate

Seunghee Seo[1)] · Taekue Hwang[2)] · Jongseong Park[2)] · Kyeongryun Park[2)] · Suhan Park[*3)]

[1)]*Department of Mechanical Engineering, Konkuk University, Seoul 05029, Korea*
[2)]*Research & Development Team, Korea Fuel-Tech Corporation, 23 Seombawi-gil, Wongok-myeon, Anseong-si, Gyeonggi 17557, Korea*
[3)]*Department of Mechanical, Robotics and Automotive Engineering, Konkuk University, Seoul 05029, Korea*
(Received 9 April 2025/ Revised 20 May 2025 / Accepted 5 June 2025)

Abstract : This study quantitatively analyzed the impact of adsorbate concentration and flow rate on adsorption efficiency, providing valuable insights into optimizing canister design for improved adsorption performance. A series of adsorption-desorption experiments was conducted using butane-nitrogen mixtures as the adsorbate. The concentration ratio of butane to nitrogen was systematically varied from 5:5 to 7:3, while flow rates were adjusted across multiple levels. The adsorption capacity and time were measured to evaluate the influence of these parameters on the activated carbon's performance. The results indicate that increasing the butane concentration enhances the adsorption capacity. At a constant flow rate, raising the butane-to-nitrogen ratio from 5:5 to 6:4 increases the average adsorption amount by 25 g (26 %) and extends the adsorption time by 29 min (21 %). Further increasing the ratio to 7:3 adds 11 g (8 %) in adsorption amount and 18 min (10 %) in adsorption time. Conversely, at a fixed butane ratio, increasing the flow rate reduces the adsorption time by 44 min (23 %), demonstrating its influence on the adsorption rate. These findings highlight that while a higher adsorbate concentration enhances adsorption capacity, flow rate plays a significant role in determining adsorption kinetics by modifying the linear velocity. Ultimately, this study provides valuable insights into optimizing the adsorption characteristics of activated carbon canisters, contributing to improved evaporative emission control in automotive applications.

Key words : Activated carbon canister, Evaporative gas, Adsorption, Breakthrough, Fixed bed adsorption system

Nomenclature

BWC : butane working capacity of activated carbon, g/100 ml
PCSV : purge control solenoid valve

1. Introduction

In line with the 2050 carbon neutrality policy, automobile emission regulations are being strengthened worldwide. The LEV4 standard, announced by the California Air Resources Board(CARB) for 2022,[1)] sets a range for non-methane organic gases and nitrogen oxides(NMOG + NOx) emissions of 0.125-0.015 g/mi and carbon monoxide(CO) emissions of 2.1-1.0 g/mi. This represents a more significant tightening compared to the previous LEV3 standard,[2)] which set a range for NMOG+NOx emissions of 0.630-0.020 g/mi and a range for CO emissions of 7.3-1.0 g/mi. With the aforementioned strengthened emission regulations, technologies to reduce fuel evaporative emissions, as well as emissions generated during fuel combustion, are becoming increasingly important. In this context, fuel evaporative emissions consist of volatile organic compounds(VOCs), which, when released into the atmosphere, can adversely affect the environment and human health. Therefore, the developing technologies that reduce fuel evaporation gas emissions appears essential. Activated carbon canisters absorb evaporative gases, preventing their release into the atmosphere, while also releasing them into the combustion chamber, thus enabling efficient fuel use. Fuel evaporative emissions primarily originate from fuel tanks and are

[*]A part of this paper was presented at the KSAE 2024 Fall Conference and Exhibition
[*]Corresponding author, E-mail: suhanpark@konkuk.ac.kr

composed of VOCs. When released into the atmosphere, VOCs not only produce unpleasant odors but also pose more risks as they contain carcinogens, such as benzene, which can be hazardous to the human body. Furthermore, they react with nitrogen oxides and ultraviolet light in the atmosphere, generating ozone through a photochemical reaction. Excessive ground-level ozone concentrations at the ground surface can negatively affect human lung health and eventually, long-term environmental issues, such as crop yield. Due to these harmful effects, fuel evaporative emissions are considered a major component of automobile exhaust. Accordingly, the emission standard was proposed to be strengthened from 2.0 g/test in EURO 6 to 1.5 g/test in EURO 7 in 2023.[3] To address these strengthened regulations, the development of hybrid electric vehicles(HEVs) and carbon-neutral fuel vehicles has been active. Hybrid vehicles and carbon-neutral fuel vehicles have various characteristics from conventional gasoline vehicles, requiring performance optimization of their components accordingly. Therefore, to optimize the performance of activated carbon canisters, a key component for reducing fuel evaporative emissions, analyzing the differences between these types of vehicles and conventional gasoline vehicles is necessary. First, hybrid vehicles differ significantly in their driving characteristics. Hybrid vehicles are divided into the popular parallel type and series-parallel type, which both use an engine and an electric motor as power sources.[4] This results in a shorter engine operating time. A specific analysis of the reduction in engine operating time can be found in Jeong.[5] The current study compared and analyzed the fuel efficiency of conventional gasoline vehicles and hybrid vehicles using the FTP-75 mode and HWFET mode fuel efficiency measurement methods. FTP-75 mode is a fuel economy measurement method for city driving, whereas HWFET mode is for highway driving. The main specifications of the vehicles used for the fuel economy measurement are as follows: Both the gasoline vehicle and the parallel HEV have a displacement of 2,359 cc, and their curb weights are almost similar at 1,530 kg and 1,680 kg, respectively. The engine outputs are 150 kW and 117 kW, respectively, so the two vehicles have the same specifications overall. The fuel economy measurement results of the two vehicles are summarized in Tables 1 and 2. The fuel economy measurement results in FTP-75 mode showed that the gasoline vehicle achieved 12.97 km/L, while the parallel HEV reached 16.88 km/L, indicating that the HEV had a 30.1 % higher fuel economy. The fuel economy measurement results in HWFET mode demonstrated that the gasoline vehicle was 19.31 km/L, and the parallel HEV was 20.43 km/L, indicating that the HEV had a 5.8 % higher fuel economy. Vehicle fuel efficiency is highly correlated with engine operating time, so engine operating time can be determined through fuel efficiency measurement items, such as idle loss (fuel loss due to engine idling when the vehicle is stopped) and engine loss (total fuel loss through heat, pumping, and accessories due to engine operation). HEVs do not exhibit idle loss because they use the electric motor instead of the engine at low speeds or when the vehicle is stopped, and engine loss is also relatively lower. Fuel efficiency measurements for idle loss and engine loss improved by 16.8 % in FTP-75 mode and a 9.2 % in HWFET mode, indicating that the engine operating time decreased proportionally to the improvement in fuel efficiency. Therefore, in HEVs, fuel evaporation gases must be stored within the canister for longer periods, making the timing of desorption critical to accommodate shorter engine operating periods.

Table 1 Results of fuel economy test -FTP-75 mode[5]

Fuel economy improvement rate [%]	FTP-75 Mode
	Parallel HEV
Idle loss	8.8
Engine loss	24.8
Electric loss	-15.9
Drivetrain + Roadload loss	9.6
Braking loss	2.7
Total	30.1

Table 2 Results of fuel economy test - HWFET mode[5]

Fuel economy improvement rate [%]	HWFET Mode
	Parallel HEV
Idle loss	0.6
Engine loss	17.8
Electric loss	-17.7
Drivetrain + Roadload loss	2.4
Braking loss	2.7
Total	5.8

Next, among carbon-neutral fuels, the commercialized ethanol-blended fuel differs most significantly in terms of

fuel volatility.[6] Ethanol's high volatility results in relatively high fuel evaporation emissions. To optimize canisters based on these fuel characteristics, enhancing adsorption performance and optimizing adsorption/desorption rates are essential. Accordingly, this study aims to identify the key factors affecting activated carbon canister performance and quantitatively evaluate the impact of each factor on performance.

In gas-phase adsorption, such as fuel evaporation, the adsorption amount increases with the adsorbate concentration (substance to be adsorbed).[7] Here, the linear velocity should be considered because securing the residence time of the adsorbate in the canister is important.[8] Studies by Lavoie et al.[9] and Romagnuolo[10] varied the flow rate and mixing ratio of the adsorbate during adsorption, analyzing and modeling the adsorption process and the change in adsorption amount according to the results. Sun et al.[11] also varied the flow rate and mixing ratio of the adsorbate and compared the test results. The previous studies' analyses confirmed that the flow rate and concentration of the fuel evaporation gas entering the canister were the most influential factors affecting canister performance.

This study performed experiments under various fuel evaporation gas inlet flow rates and fuel evaporation gas mixing ratios to determine the influence of the two factors on canister adsorption performance. In addition, by analyzing the changes in adsorption behavior under each condition, we aimed to identify which factor-adsorbate inlet flow rate or concentration primarily influences canister adsorption performance.

2. Test Apparatus and Method

The schematic diagram of an activated carbon canister installed in a vehicle is illustrated in Fig. 1. When the engine is stopped, the activated carbon canister adsorbs fuel vapor. When the engine is running, the electronic control unit(ECU) opens the purge control solenoid valve(PCSV) and the atmospheric inlet valve (canister sealing valve), sending the desorbed vapor to the intake manifold. Based on this operating process, a standard canister performance test method was established. First, during adsorption, butane and nitrogen are discharged from each gas cylinder through a flow meter according to a set flow rate. The gases mixed in an in-line mixer then flow in through the canister fuel port

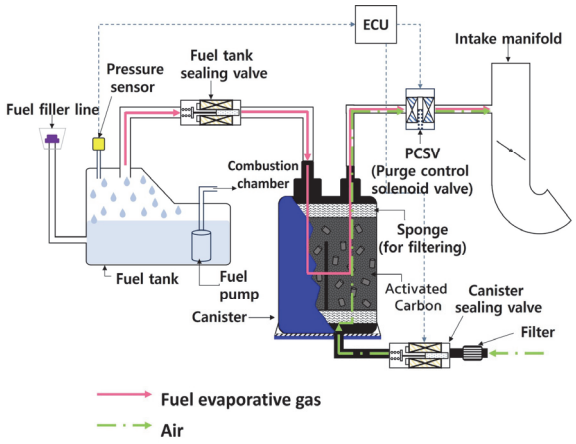

Fig. 1 Schematic of automotive canister operation

Table 3 Detailed component information of KSAE 0028

Equipment	Subject	Minimum scale	Measurement range	Accuracy
Scale	Canister	0.1 g	0 - 6000 g	± 0.1 g
	Sub Canister	0.1 g	0 - 6000 g	± 0.01 g
Mass flow meter (MFC)	N-butane & nitrogen	0.01 L/min	0 - 1.0 L/min	± 1 % FS
	Air	0.1 L/min	0 - 50 L/min	± 1 % FS

and butane is adsorbed by the activated carbon in the canister, while the nitrogen passes through the atmospheric port and flows into the auxiliary adsorption vessel. When the activated carbon in the canister reaches adsorption equilibrium, breakthrough occurs, causing butane to flow into the auxiliary adsorption vessel, where it is adsorbed by the activated carbon. The adsorption test is terminated when the auxiliary adsorption vessel shows a mass gain of 2 g. During the desorption, dry air is injected into the canister and auxiliary adsorption vessel at a flow rate controlled by a flow meter.

Air drawn in through the canister's atmospheric port expels the desorbed gas through the purge port, and the auxiliary adsorption vessel takes in air through the exhaust port and releases the desorbed gas through the supply port. To maintain constant temperature and ensure scale accuracy, the test chamber should be equipped with a granite surface plate and then the scale is placed inside. In addition, all piping and valves used in the test need to be explosion-proof, and when gasoline fuel is used as the test gas, a fuel thermostatic circulator is required. The measurement

accuracy of the test equipment specified in the standard is shown in Table 3.

The test apparatus shown in Fig. 2 was constructed according to the standard performance test methods. First, the canister test system comprises butane and nitrogen cylinders as adsorbents, mass flow controllers(MFCs) for each gas, canisters, auxiliary canisters, scales for each canister, and an MFC for atmospheric inflow. The canisters and scales were installed in a dedicated chamber for precise measurement of canister weight changes and temperature control.

For the scale, we used a product from OHAUS (Republic of Korea), with a usable range of 0-4,100 g, and an accuracy of ± 0.1 g for the canister scale and ± 0.01 g for the auxiliary canister scale. For the flow meter, HORIBA STEC (Japan) products were used for butane and nitrogen, and BRONKHORST (Republic of Korea) products were used for the atmosphere. The range of use is approximately 0.0002-500 SLM for butane and nitrogen, and the minimum is 0.014-0.7 mln/min, and the maximum is 8-1670 mln/min for the atmosphere, and the precision is ± 1 % FS for all. Since the pipes connected during the adsorption and desorption tests differ, the operating process is shown as (a) and (b) in Fig. 2. Fig. 2(a) delineates the movement path of the mixed gas of butane and nitrogen during adsorption, and the detailed process is as follows. Each gas is discharged from the butane and nitrogen cylinders, and the flow rate is controlled by the flow meter according to the given conditions. The two gases are mixed at the mixing point and then introduced through the canister gas inlet. Butane is adsorbed on the activated carbon, and nitrogen moves to the auxiliary canister through the atmosphere inlet and is then released into the atmosphere. The movement path of the mixed gas during desorption, as shown in Fig. 2(b), is as follows: Atmosphere is introduced through the atmosphere inlets connected to each of the activated carbon canisters and the auxiliary canister, and desorption proceeds. The desorbed butane is released into the atmosphere through the desorption port of each canister.

The activated carbon canister used in this test, which is prototype under development by Korea Fuel-Tech Corporation (Korea FT, Republic of Korea), has a capacity of approximately 2.1 L. The activated carbon filled in the canister was produced by the Ingevity (BAX1500). The structure of the activated carbon canister can be seen in Fig. 3, and the detailed names are as follows: There is a loading port through which fuel evaporation gas flows, a purging port through which fuel evaporation gas desorbed from the activated carbon moves to the intake manifold during desorption, and an ambient port for introducing atmosphere for desorption. There are springs and sponges near each inlet port and at the top and bottom of the canister. These secure the activated carbon, and the sponges prevent the inflow and

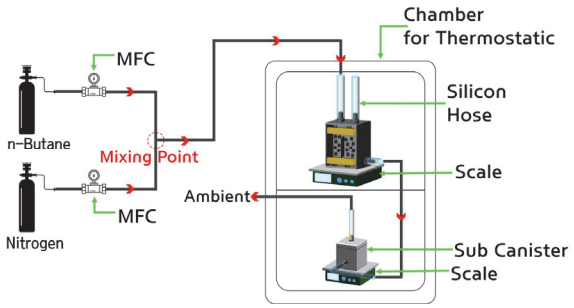

(a) Operating process of adsorption

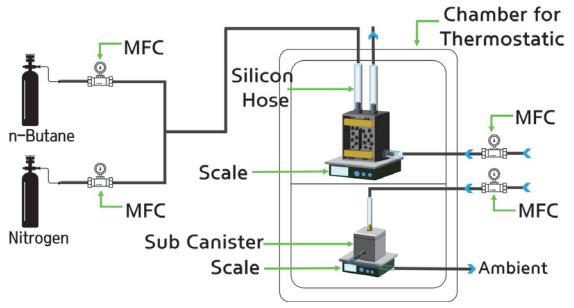

(b) Operating process of desorption

Fig. 2. Operating process of the canister experimental apparatus

Table 4 Detailed component information

Equipment	Subject	Manufacturer	Measurement range	Accuracy
Scale	Canister	Ohaus	0 - 4100 g	± 0.1 g
	Sub canister	Ohaus	0 - 4100 g	± 0.01 g
Mass flow meter (MFC)	N-butane & nitrogen	Horibastec	0.0002 - 500 SLM	± 1 % FS
	Air	Bronkhorst	*Minimum: 0.014 - 0.7 mln/min *maximum: 8 - 1670 mln/min	± 1 % FS

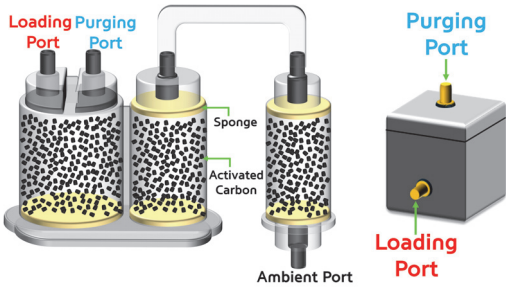

Fig. 3 Schematic of canister and sub-canister

Table 5 Canister test condition

Conditions	Value
Canister volume	2.1 L
Loading flow rate of adsorbate gas	30, 40, 50 g/hr
Loading mixing rate of the adsorbate gas (n-Butane: Nitrogen)	5:5, 6:4, 7:3, 8:2
Ambient temperature	24 - 29 °C
Humidity	47 - 60 %
Post-adsorption resting phase	3 min
Bed volume	300
Breakthrough	2 g
Purging flow rate	25 L/min

outflow of impurities such as activated carbon powder.

Table 5 lists the test conditions, where the main conditions are the mixing ratio and flow rate of the butane and nitrogen mixture gas supplied to the canister during adsorption. The mixing ratio of butane and nitrogen was classified into four types: 5:5, 6:4, 7:3, and 8:2, and the adsorbate inflow flow rate was classified into three types: 30 g/hr, 40 g/hr, and 50 g/hr. The outside temperature and humidity were set according to the climate during the actual test, but the range of change was limited to within the provided constant values. In order to minimize the influence of the previous cycle after one cycle (adsorption-rest-desorption), a pre-desorption process was added before adsorption, and this pre-desorption volume was set to 5000 BV.

The actual supply flow rate of the butane-nitrogen mixed gas supply according to the main test conditions, namely the adsorbent inlet flow rate and mixing ratio, is shown in Fig. 4. In this test, the adsorbate for the activated carbon adsorbent was limited to butane, so the test conditions were satisfied by controlling the flow rate of butane. The reason

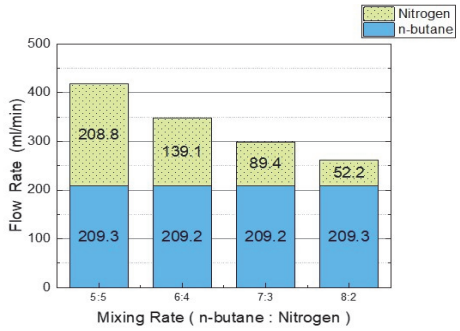

(a) Respective flow rates of the adsorbates at 30 g/hr

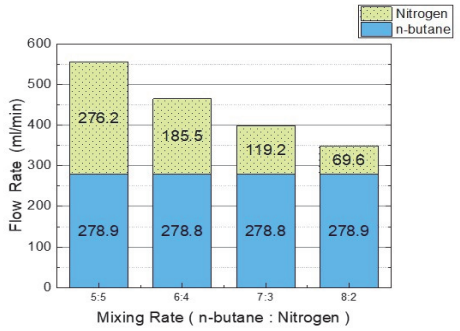

(b) Respective flow rates of the adsorbates at 40 g/hr

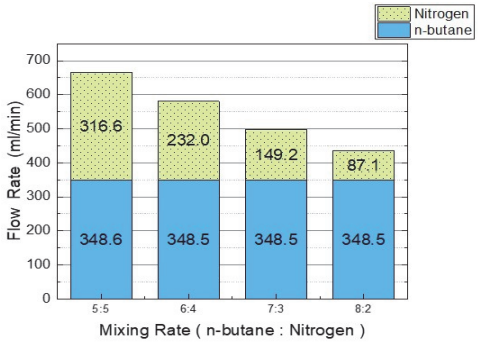

(c) Respective flow rates of the adsorbates at 50 g/hr

Fig. 4 Respective flow rates under various flow conditions and mixing rates

that only butane is considered as the adsorbent is as follows: the adsorption process for a binary mixed gas consisting of butane and nitrogen occurs through competitive adsorption, in which the component that is strongly adsorbed during single adsorption is also strongly adsorbed during competitive adsorption. Strong adsorption requires a large molecular weight and intermolecular attraction, and the same polarity (nonpolarity) as the adsorbent, activated carbon. The molecular weight of butane is 58.12 g/mol and nonpolar, whereas the molecular weight of nitrogen is 28.01

g/mol and polar. In addition, since butane has a boiling point of -0.5 ℃ and nitrogen has a boiling point of -195 ℃, butane has a higher boiling point, and the intermolecular attraction is stronger. Therefore, among the two components, only butane is primarily adsorbed; hence, only butane was considered as the adsorbate. In addition, since the mixing ratio was to examine the concentration of butane in the mixed gas flowing into the canister, the mixing amount of nitrogen was adjusted to meet the ratio.

The detailed test method is as follows: First, based on the flow rate and mixing ratio of the adsorbent set during adsorption, the flow rates of butane and nitrogen are determined and supplied at the corresponding flow rates from the MFC. This mixed gas passes through the canister inlet, where butane is adsorbed on the activated carbon inside the canister, while nitrogen is not adsorbed and flows into the auxiliary canister through the atmosphere inlet. Afterward, if the mixed gas is continuously supplied, the activated carbon adsorption layer of the canister reaches saturation, reaching equilibrium with the adsorbent concentration at the adsorption port. If the adsorbent is further supplied, butane cannot be further adsorbed on the activated carbon, resulting in a breakthrough. The butane gas flows into the auxiliary canister. Consequently, butane adsorption progresses on the activated carbon of the auxiliary canister, causing the weight of the auxiliary canister to increase. When this weight reaches 2 g, adsorption is terminated. After a 3-minute pause, desorption is performed. Desorption is done by introducing outdoor air through the atmosphere inlet of the canister. Butane physically adsorbed on the activated carbon inside the canister is desorbed through pressure changes and released through the desorption port. Desorption ends when the set desorption volume of 300 BV is reached. When the entire adsorption-rest-desorption process is performed once, it is considered one cycle, and three cycles were performed for each condition. The test data mainly used for analysis in this test were the adsorption time (the time for the increase value of the auxiliary canister to reach 2 g during adsorption) and the change in increase in the main and auxiliary canisters during adsorption, the desorption time, and the change in weight loss during the process of desorption. The final results of the test data for each condition used the average value of the second and third cycles out of the three cycles performed.

3. Test Results and Discussion

Fig. 5 shows the change in total adsorption (Total Loading Mass) when varying the butane ratio in the mixed gas under the same flow rate. Under the same flow rate, the total adsorption increased as the butane ratio increased. The average increase and rate of increase in total adsorption as the butane ratio increased under the same flow rate were as follows. When the butane-to-nitrogen mixing ratio increased from 5:5 to 6:4, the total adsorption increased by approximately 25 g (26 %). When the butane-to-nitrogen mixing ratio increased from 6:4 to 7:3, the total adsorption increased by approximately 9 g (7 %). When the butane-o-nitrogen mixing ratio increased from 7:3 to 8:2, the total adsorption increased by approximately 12 g (9 %).

Conversely, the average increase in total adsorption with flow rate was minimal. To verify this, the standard deviation

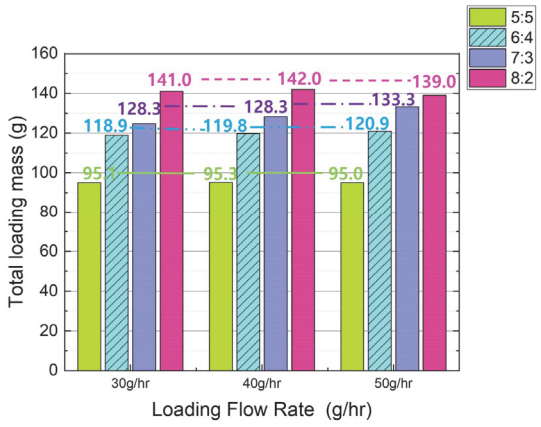

Fig. 5 Total loading mass under varying ratios at the same flow rate condition

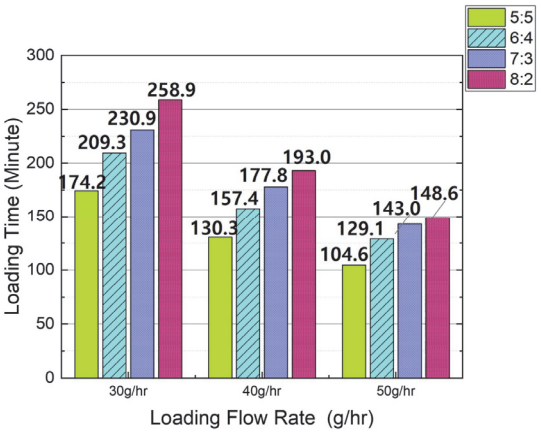

Fig. 6 Loading time under varying ratios at the same flow rate condition

of total adsorption was calculated for each butane-to-nitrogen mixing ratio and flow rate. When the mixing ratio of butane and nitrogen was 5:5, the average total adsorption amount by flow rate was approximately 95 g, and the standard deviation was 0.1 g. When the mixing ratio was 6:4, the average total adsorption amount by flow rate was approximately 120 g, and the standard deviation was 1.0 g. When the mixing ratio was 7:3, the average total adsorption amount by flow rate was approximately 129 g, and the standard deviation was 4.2 g. When the mixing ratio was 8:2, the average total adsorption amount by flow rate was approximately 141 g, and the standard deviation was 1.6 g. Therefore, it can be expected that the flow rate of the adsorbate has a minimal effect on the total adsorption amount under each mixing ratio condition, and that the flow rate is not a crucial factor significantly affecting the canister adsorption capacity.

Fig. 6 shows the change in adsorption time according to the increase in the mixed gas ratio under the same flow rate conditions. As detailed in Fig. 6, the adsorption time increased as the butane ratio increased, and the average increase rate of adsorption time when the butane ratio increased under each flow rate condition is as follows. When the butane to nitrogen ratio increased from 5:5 to 6:4, the average adsorption time increased by approximately 29 minutes (21 %). When the butane to nitrogen ratio increased from 6:4 to 7:3, the average adsorption time increased by approximately 19 minutes (11 %). When the butane to nitrogen ratio increased from 7:3 to 8:2, the average adsorption time increased by approximately 16 minutes (8 %).

This result confirmed that an increase in the butane ratio in the mixed gas was a major factor in both the adsorption amount and the adsorption time. This can be further confirmed by the Butane Working Capacity(BWC) shown in Fig. 7. The BWC is an indicator of adsorbent performance, which represents the amount of butane that the adsorbent can actually adsorb through adsorption and desorption. The BWC was calculated using the formula in the Standard for Canister Performance Test Methods.[18)]

$$\frac{((Canister\ weight\ after\ adsorption)-(Canister\ weight\ measured\ before\ adsorption)\,[g])}{((\text{Activated carbon volume filled} \in \text{the canister}\,[ml]))} \quad (1)$$

Fig. 7 suggests that, under the same flow rate conditions, the BWC increases as the mixing ratio of butane increases. On the other hand, even when the flow rate changes at the same mixing ratio, the BWC remains nearly constant. Therefore, it can be confirmed that an increase in the butane ratio in the mixed gas is indeed a major factor in increasing the adsorption amount and the adsorption time.

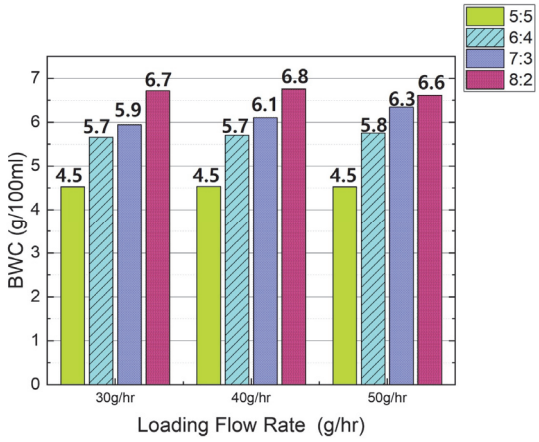

Fig. 7 Increase in butane working capacity of canister with higher butane mixing ratio under the same flow conditions

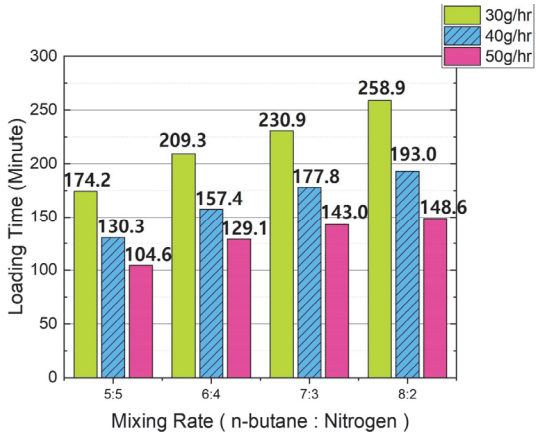

Fig. 8 Loading time under varying flow rate at the same ratio condition

Fig. 8 shows the change in adsorption time when the flow rate was varied under the same butane mixing ratio conditions. The test results verified that the adsorption time tended to decrease as the flow rate increased. The average adsorption time reduction rate is as follows: When the flow rate increased from 30 g/hr to 40 g/hr, the average reduction time was approximately 54 minutes, representing an average reduction rate of 25 %. When the flow rate increased from 40 g/hr to 50 g/hr, the average reduction time was approximately 33 minutes, representing an average reduction rate of 20 %.

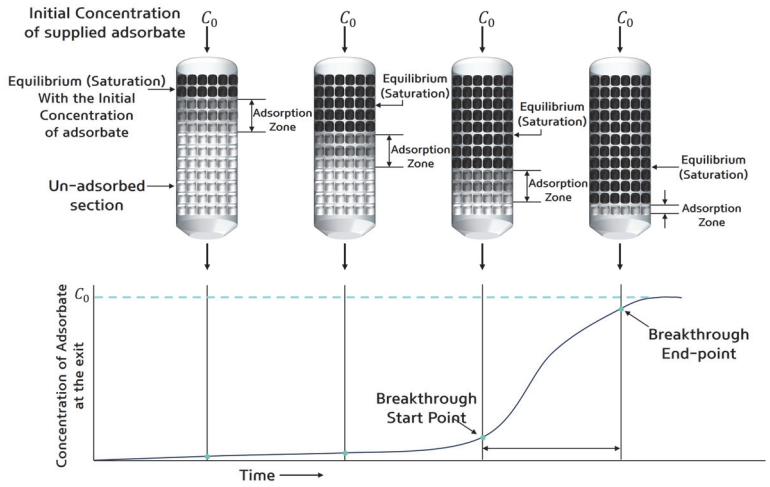

Fig. 9 Adsorption process and breakthrough curve of fixed-bed adsorption systems[8)]

The results of Figs. 5 ~ 8 are summarized as follows: As the concentration of butane increases, both the total adsorption amount and the adsorption time of the canister increase, indicating that the concentration of the adsorbate is a major factor in the adsorption capacity of the activated carbon canister. This finding can be explained using the principle of the fixed-bed adsorption system, as in Fig. 9. The fixed-bed adsorption system mainly refers to an industrial activated carbon adsorption tower, but its operating method is similar to that of an automotive activated carbon canister, so its principle is applied. First, the adsorption method of the fixed-bed adsorption system is classified into the saturation process and the elution chromatography method. Among them, adsorption in the automotive canister is performed using the saturation process. The characteristics of the fixed-bed adsorption system are that a breakthrough curve appears, and an adsorption zone (mass transfer zone) is formed during adsorption. The adsorption zone refers to the area where adsorption occurs. The upper part of the adsorption zone is in equilibrium with the adsorbate concentration at the device inlet, so it can be considered as a saturated state where adsorption is complete, and the lower part of the adsorption zone is viewed as a preliminary adsorption zone where adsorption has not yet occurred. If the adsorbate is continuously supplied to the adsorption zone, the adsorption zone will reach equilibrium with the adsorbate concentration at the device inlet over time. When the activated carbon adsorption zone reaches saturation, the adsorption capacity decreases rapidly, and adsorption occurs

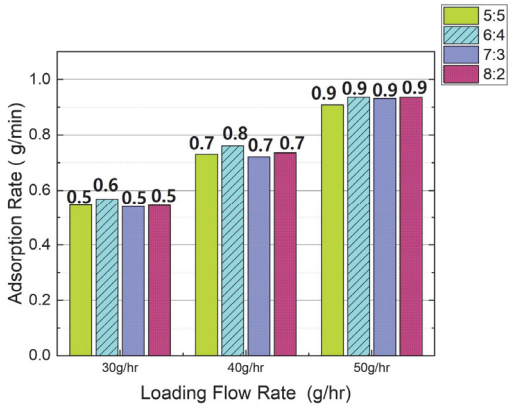

Fig. 10 Similar adsorption rate at different flow rates

primarily in the unsaturated lower part. This process allows the adsorption zone to gradually move downward and reach the bottom of the adsorption zone, where the adsorbate gradually flows out, and the breakthrough begins. The breakthrough start point is when the adsorbate concentration detected at the canister outlet reaches 5-10 % of the adsorbate concentration at the device inlet. The curve that shows the process over time from the breakthrough start point to the end of adsorption is called the breakthrough curve. According to the principle of this fixed-bed adsorption device, as the butane concentration in the butane and nitrogen mixture flowing into the canister increases, the total adsorption amount available to the adsorption layer increases. Furthermore, as shown in Fig. 10, when the flow rate is constant, the adsorption rate is also constant at all butane mixing ratios.

If adsorbate concentration is the primary factor in adsorption, then adsorbate flow rate is the main factor determining the adsorption rate. The results in Fig. 5 and Fig. 8 confirm that, at the same mixing ratio, adsorption time decreases as the flow rate increases, but the total adsorption amount remains generally constant. This is because, as shown in Fig. 8, as the adsorbate flow rate increases, both adsorption time and adsorption rate increase. This increase in adsorption rate with increasing flow rate is due to the increase in linear velocity of the adsorbate by the increased flow rate. In a fixed-bed adsorption device, linear velocity can be calculated by dividing the gas inflow rate by the cross-sectional area of the adsorbent, as in Equation (2).

Linear velocity of adsorbate =
Gas inflow rate [m^3/sec] ÷ Adsorbent cross-sectional area [m^2] (2)

Next, the relationship between the flow rate, linear velocity, and adsorption rate can be interpreted through the adsorption principle of activated carbon, a porous adsorbent. The adsorption process of activated carbon can be summarized into three stages.[8] The first stage is diffusion from the bulk of the adsorbate to the boundary layer of the activated carbon, which is the adsorbent, and this boundary layer is formed by the principle of viscous flow. In the second stage, the adsorbate passes through this boundary layer and diffuses from the macropores (≥50 nm) of the adsorbent to the mesopores (2-50 nm). In the third stage, the adsorbate that has moved from the mesopores is adsorbed on the inner surface of the micropores (≤2 nm). Particularly, the diffusion patterns in stages 2 to 3 can be divided into two types: The first is serial diffusion, which is diffusion from the bulk of the adsorbate in the macropores to the mesopores. Next, surface diffusion first diffuses from the boundary layer to the macropore walls, adsorbs at the adsorbed site, and then diffuses to adjacent intermediate pores for subsequent adsorption. Subsequently, adsorption into micropores occurs similarly. Surface diffusion requires more time because the adsorbed molecules must move, and surface diffusion occurs more frequently during the actual adsorption process. The diffusion rates at each activated carbon adsorption stage are slow in the first and second stages, while the micropore surface adsorption in the third stage proceeds rapidly.

The adsorption rate of these activated carbon pores is affected by the flow rate of the adsorbate. As the flow rate of the adsorbate increases, the linear velocity increases, leading to a more consistent path for the adsorbate gas within the canister. This relatively increases the concentration gradient, facilitating the smooth diffusion of the first stage of the adsorption process (Fick's law 1st). Furthermore, as the linear velocity increases, the boundary layer of the activated carbon becomes thinner based on viscous flow and the Reynolds number. This accelerates the second stage of diffusion. Consequently, the adsorption rate increases relatively, shortening the adsorption time, resulting in a more ideal breakthrough curve. Conversely, as the flow rate decreases, the linear velocity slows, promoting the active dispersion of the adsorbate gas within the canister. Therefore, this lowers the concentration gradient, slowing down the first stage of the adsorption process. Accordingly, the adsorption rate slows down and the overall adsorption time also becomes longer. At the same time, the shape of the breakthrough curve deviates from the ideal, appearing gentle.

Additionally, to verify the applicability of this theory to actual adsorption processes, the Reynolds number was calculated using experimental results.

$$Re = \frac{\rho V L}{\mu} \tag{3}$$

The Reynolds number is defined by Equation (3). The values required for this equation were derived from the experimental conditions of a 5:5 mixing ratio and flow rates of 30 g/hr, 40 g/hr, and 50 g/hr. The density (ρ) was assumed to be 2.37 kg/m^3 of butane gas at the average ambient temperature of 25°C. The velocity (V) was calculated using the linear velocity of butane, depending on the flow rate, which was calculated using the linear velocity equation mentioned above. The length (L) of the object is the circular diameter of the pellet-shaped activated carbon packed in the canister used in the test, which is 0.0022 m. The cross-sectional area of the adsorption tower is 0.0133 m^2. The viscosity coefficient (μ) was 7.41×10^{-6} kg/m・sec, reflecting the test conditions (1 atm, 25℃). Detailed values for each item are summarized in Table 6.

The Reynolds number for each flow rate condition at a 5:5 mixing ratio was calculated to be 0.185 at 30 g/hr, 0.246

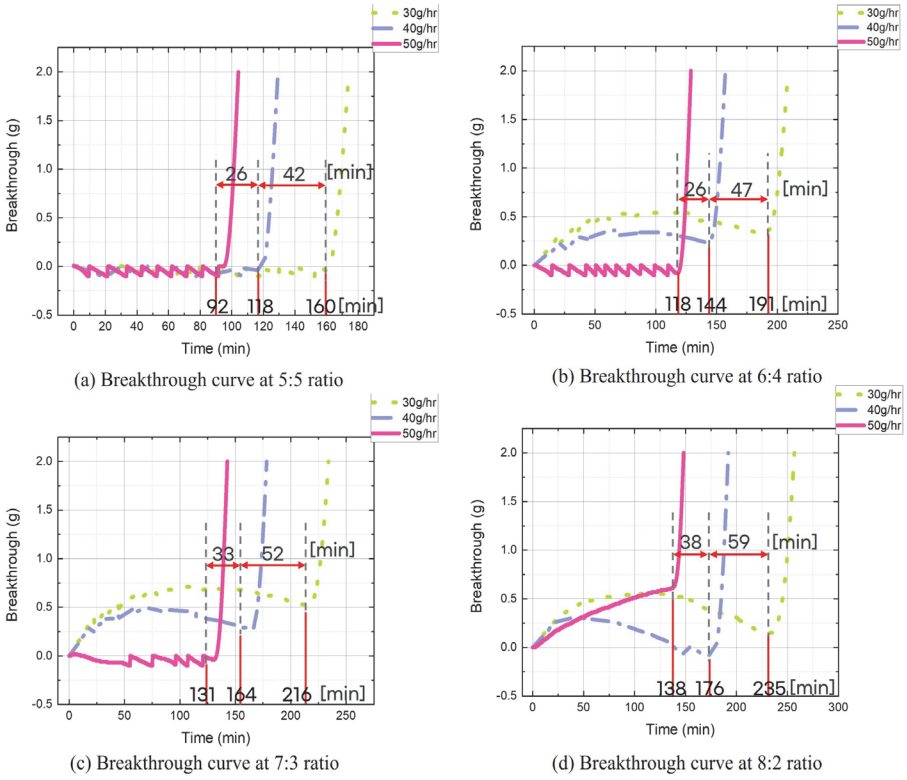

Fig. 11 Breakthrough curve at various ratios

Table 6 Reynolds number

Flow rate →	30 g/hr	40 g/hr	50 g/hr
Linear velocity [m/sec]	2.63×10^{-4}	3.5×10^{-4}	4.38×10^{-4}
Reynolds number	0.185	0.246	0.308

at 40 g/hr, and 0.308 at 50 g/hr. The Reynolds number increase rate according to the increase in flow rate is about 33 % (1.33 times) when increasing from 30 g/hr to 40 g/hr, about 25 % (1.25 times) when increasing from 40 g/hr to 50 g/hr, and about 66 % (1.66 times) when increasing from 30 g/hr to 50 g/hr. As the flow rate increases at the same rate as the Reynolds number increases, the thickness of the adsorbate boundary layer on the activated carbon surface also becomes thinner, narrowing the viscous flow region. As a result, the boundary layer resistance decreases, and the diffusion rate from the boundary layer to the internal pores of the activated carbon becomes faster.

Fig. 11 presents that, under the same ratio conditions, the lower the flow rate, the more the breakthrough curve deviates from the ideal shape. Specifically, comparing the breakthrough curves for butane:nitrogen ratios of 6:4 and 8:2 at a flow rate of 50 g/hr reveals that as the butane concentration increases, the ideal breakthrough curve shape is achieved at a higher flow rate. This phenomenon is attributed to the fact that as the concentration of the adsorbate butane increases, more butane exists inside the canister, thickening the butane boundary layer on the activated carbon surface. When the boundary layer thickens, the initially slow first stage of the adsorption process slows down further, according to the adsorption stage-by-stage rate described above, reducing the overall adsorption rate. Consequently, the adsorbate butane floats inside the canister without being rapidly adsorbed by the activated carbon, leaking along with the nitrogen flowing through the canister. Therefore, to reduce boundary layer resistance and achieve an ideal breakthrough curve, the adsorbate flow rate must also increase as the adsorbate concentration increases.

4. Conclusion

This study analyzed the changes in the adsorption process of activated carbon canisters through canister adsorption and desorption experiments in which the adsorbate flow rate and mixing ratio were varied. The following conclusions were

drawn from the findings:

1) Under the same flow rate conditions, total adsorption increased as the butane ratio in the mixed gas increased. The average increase in total adsorption was approximately 26 % (25 g) when the butane:nitrogen ratio increased from 5:5 to 6:4, and approximately 8 % (10 g) for subsequent increases.
2) Under the same flow rate conditions, the adsorption time increased with a higher butane ratio in the mixed gas. The average increase was 21 % (29 min) when the butane: nitrogen ratio increased from 5:5 to 6:4 and approximately 10 % (18 min) for further increase.
3) At a constant butane mixing ratio, the adsorption time decreased as the flow rate increased. The average adsorption time decreased by 23 % (44 min) with increasing flow rate.
4) Adsorption rate increased with increasing flow rate. At 30 g/hr, the average adsorption rate was 0.53 g/min; at 40 g/hr, it was 0.73 g/min; and at 50 g/hr, it was 0.9 g/min.
5) At low adsorbate flow rates, the linear velocity was reduced, resulting in a looser, less ideal breakthrough curve. On the other hand, at high adsorbate flow rates, the linear velocity increased, resulting in a more ideal breakthrough curve.

Acknowledgements

This study was supported by research grants from the Ministry of Trade, Industry and Energy and the Korea Evaluation Institute of Industrial Technology(KEIT) (200-18834). The authors would like to thank the supporting organizations.

References

1) California Air Resources Board, “Exhaust Emission Standards and Test Procedures-2026 and Subsequent Model Year Passenger Cars, Light-Duty Trucks, and Medium-Duty Vehicles,” Section 1961.4, 2022.
2) California Air Resources Board, LEV III: Amendments to the California low-emission vehicle regulations, https://ww2.arb.ca.gov/our-work/programs/advanced-clean-cars-program/lev-program/low-emission-vehicle-lev-iii-program, 2025.
3) European Commission. Commission welcomes political agreement on the Euro 7 regulation. European Commission. https://single-market-economy.ec.europa.eu/news/commission-welcomes-political-agreement-euro-7-regulation-2023-12-19_en, 2023.
4) D. Kim, J. Park, S. Jo and C. Kim, “Thematic Planning for Power Transmission Systems and Control Technologies for Hybrid Electric Vehicles,” Journal of the KSME, Vol.42, No.9, pp.36–40, 2002.
5) I. C. Jung, Analysis of fuel economy of HEV on real road driving, Master. Dissertation, Ajou University, Suwon, 2015.
6) K. Noh, M. Lee, K. Kim, S. Kim and C. Park, “The Characteristics Study of Vehicle Evaporative Emission and Performance according to the Bio-Fuel Application,” KSAST, Vol.34, No.4, pp.874–882, 2017.
7) Y. Park, New Edition of Activated Carbon: Basics and Applications, Donghwa Technology Co. Ltd, Paju-si, pp.153, 1992.
8) J. Lim, Adsorption Science and Engineering and Adsorbents, Naeha Publishing House, Seoul, p.135, 2012.
9) G. A. Lavoie, P. J. Johnson and J. F. Hood, “Carbon Canister Modeling for Evaporative Emissions: Adsorption and Thermal Effects,” SAE Transactions, pp.1028–1049, 1996.
10) L. Romagnuolo, E. Frosina, F. Fortunato, A. Andreozzi and A. Senatore, “1D Model for N-butane Adsorption and Thermal Variation for EVAP Canister of Gasoline-Fueled Vehicles: Validation with Experimental Results and DFSS Optimization,” Applied Thermal Engineering, Vol.209, Paper No. 118267, 2022.
11) J. Sun, Z. Yang, D. Peng, C. Zhong, T. Zhang and Z. Li, “Experimental Study on Working Capacity of Carbon Canister Based on Euro VI,” EDP Sciences, Vol.360, Paper No.01022, 2022.
12) L. Romagnuolo, R. Yang, E. Frosina, G. Rizzoni, A. Andreozzi and A. Senatore “Physical Modeling of Evaporative Emission Control System in Gasoline Fueled Automobiles: A Review,” Renewable and Sustainable Energy Reviews, Vol.116, Paper No. 109462, 2019.
13) P. J. Johnson, J. R. Jamrog and G. A. Lavoie, “Activated Carbon Canister Performance during Diurnal Cycles: An Experimental and Modeling Evaluation,” SAE Transactions, pp.582–592, 1997.
14) P. Girardi, A. Gargiulo and P. C. Brambill, “A Comparative LCA of an Electric Vehicle and an Internal Combustion Engine Vehicle Using the Appropriate Power Mix: The Italian Case Study,” The International Journal of Life Cycle Assessment, Vol.20, pp.1127–1142, 2015.

15) J. Park, Y. Park, Y. Lim, J. Lee, J. Kim and K. Choi, "A Study on the Evaporative Emission Characteristics of Korean Gasoline Vehicles," Transactions of KSAE, Vol.19, No.4, pp.121–129, 2011.
16) S. Jeong and W. Kim, "Three-Dimensional Fluid Flow Analysis of Automotive Carbon Canisters for Reducing Evaporative Emissions," Transactions of KSAE, Vol.9, No.6, pp.85–93, 2001.
17) J. Lee, G. Yong, C. Kim and S. Eom, "The Study on Characteristic of Vehicle Greenhouse Gas Emission Applying Real Road Driving," Journal of Auto-vehicle Safety Association, Vol.10, No.3, pp.45–54, 2018.
18) Korean Society of Automotive Engineers Standard, KSAE 0028: Performance Test Methods of Canisters for the Automobile, 2022.
19) S. Verma, G. Dwivedi and P. Verma, "Life Cycle Assessment of Electric Vehicles in Comparison to Combustion Engine Vehicles: A Review," Materials Today: Proceedings, Vol.49, pp.217–222, 2022.
20) M. Y. Park, C. Y. Cho and Y. S. Park, "LEV-3 Environmental Regulations Corresponding Studies on the Effects on the Evaporative Emissions from the Fuel System Caused a Secondary Canister," KSAE Spring Conference Proceedings, pp.140–146, 2016.
21) G. S. Cho, Y. J. Jung and H. K. Jin, "Development of Carbon for Refueling Vapor Recovery of Vehicle (In the case od analysis of air flow in the canister)," KSAE Spring Conference Proceedings, pp.231–236, 2002.
22) S. H. Park, W. Kang, J. W. Min, J. K. Kim and M. Y. Park, "Study on the Performance Enhancement of Canister," KSAE Spring Conference Proceedings, pp.573–578, 2006.
23) S. H. Seo, S. H. Park, T. K. Hwang and J. S. Park, "Study on Adsorption and Desorption Characteristics, and Development of Prediction Model of Automotive Canister," KSAE Annual Conference Proceedings, pp.207–208, 2024.
24) C. Kim, Latest Series in Automotive Engineering 5: Electronic Fuel Injection System (Gasoline), Golden-Bell Corp, Seoul, p.173, 2011.
25) D. J. Kim, G. S. Lee, H. C. Kim, H. S. Heo, B. C. Na, S. B. Choi, W. Y. Ra and Y. S. Cho, "Butane Working Capacity Evaluation of HC Adsorption Filter for Evaporative Gas to Satisfy PZEV Regulation," Transaction of KSAE, Vol.17, No.4, pp.133–138, 2009.